

Refined characterization of head and neck squamous cell carcinomas expressing a seemingly wild-type p53 protein

Katharina Leng, Simone Schlien, Franz X. Bosch

Molekularbiologisches Labor, Universitäts-HNO-Klinik, Heidelberg, Germany

BACKGROUND: A fraction of head and neck squamous cell carcinomas (HNSCC) reveal overexpression of the p53 protein although sequence analysis failed to detect mutations in the core region of the protein. The functional and clinical status of p53 in these tumors is unclear.

METHODS: In 31 HNSCC, allelic imbalances (AI) at TP53 and other chromosome 17 loci were analyzed by microsatellite marker analysis. Expression of p16^{INK4a} protein was analyzed by immunohistochemistry. Seven tumors were re-examined for sequence alterations by the Affymetrix p53 GeneChip.

RESULTS: About 54.8% of these tumors showed AI at TP53; 41.9% showed loss of p16, an overlapping fraction of 35.5% demonstrated AI and p16 loss. Six of seven such tumors revealed heterozygous missense mutations.

CONCLUSIONS: A large proportion of HNSCC with presumed wild-type p53 overexpression are false-negative cases. These results strengthen the established strong association of p53 protein overexpression with missense mutations. AI at TP53 and p16 loss are useful surrogate markers for genetic alterations of TP53 in HNSCC.

J Oral Pathol Med (2006) 35: 19–24

Keywords: allelic imbalances; head and neck cancer; mutation and expression; p16^{INK4a} protein; p53

Introduction

Head and neck squamous cell carcinoma (HNSCC) is amongst the most devastating tumor types, because it affects vital organ functions such as speech, breathing, and swallowing. Despite constant improvements in therapeutic approaches over recent years, survival rates have not changed accordingly (1). Most likely, this failure to improve survival is due to the heterogeneous biologic

and clinical behavior, as reflected in a high variability of local tumor recurrences, second primary carcinomas, lymph node metastasis, and metastasis to distant organs. This heterogeneity is maintained even in subentities of HNSCC derived from the different anatomical sites oral cavity, oropharynx, hypopharynx, and larynx. In turn, this heterogeneous behavior points to different molecular pathogenetic pathways.

Development and progression of human cancers including HNSCC is a multistep process of genetic alterations. Among the multitude of factors underlying carcinogenesis of HNSCC, disturbance of the function of p53 tumor-suppressor protein is regarded as one of the most important events, as wild-type p53 protein would inhibit tumor growth (2). The most common mechanism of p53 inactivation is missense mutation within exons 5–8 of the gene which encode the core domain of the protein, and most, but not all of these results in accumulation (overexpression) of the p53 protein. Consequently, a good statistical correlation has been observed between accumulated p53 protein and missense mutations (3, 4), and between lack of p53 protein and nonsense mutations (4). In contrast, the relationship between mutations and the allelic status of the p53 gene is more complex. While in most tumors displaying allelic imbalance (AI) or loss of heterozygosity (LOH) at the TP53 locus and other loci on chromosome 17 as determined by allelotyping analysis, gene mutations are detectable by sequence analysis, only about half of the tumors with missense or nonsense mutations in sequence analysis display AI or LOH in subsequent allelotyping. This discrepancy is explained by the dominant negative nature of a large fraction of mutations (the so-called structural mutations in particular, see Ref. 5) over the wild-type protein, thus obviating the need for deletion of the wild-type allele. Many other mutations, however, do not exert such dominant negative effects on the wild-type protein and are therefore accompanied by wild-type allele deletion.

The AI/LOH has been examined in many studies as a surrogate marker for mutation, and has consistently been found to occur very early in HNSCC development (6). The validity of this concept has recently been strongly supported in a study on HPV-associated HNSCC in which p53 function is impaired by the E6 oncoprotein of high risk HPV (mostly HPV16), in

Correspondence: Franz X. Bosch, Molekularbiologisches Labor, Universitäts-HNO-Klinik, Im Neuenheimer Feld 400, D-69120 Heidelberg, Germany. Tel.: +49 (0) 6221/567278. Fax: +49 (0) 6221/564604. E-mail: franz_bosch@med.uni-heidelberg.de
Accepted for publication August 10, 2005

comparison with HNSCC expressing a mutated p53 protein. While the latter group showed AI (LOH) at TP3 and surrounding loci in the vast majority of cases, no imbalances at all were observed in the HPV-associated tumors (7).

Although sequence analysis is the most accurate method to determine the genetic status of p53, also it may well be the least sensitive method. This applies especially to the currently employed fluorescence-based semiautomated techniques (8), as has been also employed in our recent large-scale study (4). The rate of false-negative cases (no mutations detected but tumors actually mutated) is unclear as is the rate of false-positive cases associated with RNA sequencing approaches (9). We have therefore decided to tackle this question specifically in a small cohort of tumors, which expressed the p53 protein to various extents but were seemingly wild type by conventional sequence analysis. We analyzed the allelic status of a panel of microsatellite marker regions on chromosome 17 including the *TP53* locus itself. In addition, we also analyzed protein expression of the cyclin-dependent kinase inhibitor p16^{INK4a}, because in a large-scale study employing tissue microarray immunohistochemistry (IHC) we have obtained indirect evidence that loss of expression of p16^{INK4a} might be linked with p53 alterations (S. Karsai, A. Affolter, A. Grüttgen, S. Schlien, S. Joos, C. Hofak, F. Bosch, personal communication). If this hypothesis were valid then p16 loss should also be associated with AIs. Possible false-negative cases for p53 mutations were resequenced using the *p53 GeneChip* from Affymetrix (Affymetrix, Santa Clara, CA, USA) which provides information on all protein coding exons 2–11 as well as intronic sequences and which was found to be more sensitive than dideoxy sequencing in mutation detection (for a detailed description, see Ref. 8, 10, 11) Our results showed that semiautomated conventional sequencing indeed yielded a substantial fraction of false-negative cases. Consequently, there is an even better correlation between p53 overexpression and genetic alteration, than recognized previously. Allelic imbalances at and around the *TP53* locus, especially in conjunction with loss of p16, are useful surrogate markers for genetic alterations of *TP53* in tumors with p53 protein expression.

Material and methods

Patients and biopsy material

From a previous study on a larger cohort of patients suffering from SCC of the head and neck, 31 primary tumors were selected. These tumors had shown a various degree of expression of the p53 protein in IHC. Upon DNA sequencing of the p53 gene, no mutations could be found in any of these tumors. Some frozen tissue to be used for the DNA microsatellite marker analysis, and paraffin-embedded tissue sections for immunohistochemical analysis remained available.

DNA extraction and allelotype analysis by PCR

Tumor tissue was manually microdissected away from stroma using frozen sections lightly counterstained with

hematoxylin. As normal control tissues from the same individuals, connective tissue or muscle tissue was dissected either from separate biopsies or, if feasible, from the tumor sections. DNA was extracted using a QIAmp DNA Mini Kit (Qiagen, Hilden, Germany) according to the manufacturer's protocol.

Polymerase chain reaction (PCR) was performed to amplify the DNA regions defined by the microsatellite primers in a total volume of 10 µl, containing 1 µl DNA and 15 µM of each specific primer set. We used the ABI linkage mapping sets, Panels 23 and 24 (ABI Perkin Elmer, Weiterstedt, Germany) to cover 13 microsatellite markers on chromosome 17 (Table 1). The amplification included 30 cycles of denaturation at 94°C respectively, 89°C for 20 s, annealing at 55°C for 35 s and elongation at 72°C for 20 s with a hot start at 95°C for 3 min. The resulting DNA fragments were analyzed by automated fluorescence detection using the Gene Scan analysis software (GENESCAN 2.1, ABI, Norwalk, CT, USA) on an ABI-Prism 310 Genetic Analyzer. After identification of informative cases, i.e. allelic peaks showing heterozygosity, AIs was defined as ≥40% difference of the ratio of peak heights between neoplastic tissues and non-neoplastic controls.

Immunohistochemistry (IHC)

After the tissue sections were deparaffinized and rehydrated, antigen retrieval was performed by boiling for 10 min in 10 mM citrate buffer (pH 6.0). Endogenous peroxidase was inactivated with 3% hydrogen peroxide for 10 min, non-specific antibody binding was blocked with goat serum [Dianova, Hamburg, Germany; diluted at 1:10 with phosphate-buffered saline (PBS)] for 1 h. Incubation with the primary antibodies was at 4°C overnight. The applied antibodies were mouse anti-p53 monoclonal antibody Bp53-12 (diluted 1:8000) and mouse anti-p16 monoclonal antibody DSC 50.2 (diluted 1:10; both antibodies were subclass immunoglobulin G (IgG) and were obtained from Progen, Heidelberg, Germany). Biotinylated goat antimouse (Dianova; subclass IgG, diluted 1:1000) was used as secondary antibody (incubated for 30 min at room temperature). For detection, reagents from the ABC kit (Vector, Burlingame, CA, USA) and diaminobenzidine (DAB)

Table 1 Microsatellite markers used for allelotyping

Name	5'-Modification	MgCl ₂ concentration (mM)	Amplified DNA fragments (bp)
D17S849	TET	1.5	250–262
D17S938	FAM	1.5	234–254
TP53	HEX	1.5	103–135
D17S945	FAM	1.5	295–321
D17S799	HEX	1.5	182–202
D17S925	HEX	2.5	150–168
D17S798	HEX	1.5	292–316
D17S791	HEX	1.5	239–279
D17S787	TET	1.5	134–170
D17S808	TET	2.0	327–341
D17S949	FAM	1.5	207–223
D17S802	TET	2.0	165–189
D17S784	HEX	1.5	225–239

as chromogene substrate (Vector) were used. The sections were counterstained with methyl green or hematoxylin.

Tyramide signal amplification-IHC

For increasing the sensitivity of detection of the p16^{INK4a} protein by IHC, the tyramide signal amplification (TSA) System (NEN, Boston, MA, USA) was used. After reaction with the primary and secondary antibody and washing, the sections were incubated with the streptavidin-horseradish peroxidase (HRP) complex (NEN; diluted at 1:100) for 30 min, and then with the biotinylated tyramide, 1:50 diluted in amplification diluent. After washing, the standard staining procedure was performed, using the reagents of the ABC kit (Vectastain; Vector Laboratories) and DAB (Vector Laboratories). Precipitate development of the DAB substrate solution was monitored under the microscope. The sections were counterstained with methyl green or hematoxylin.

Evaluation of immunohistochemistry

Immunohistochemical reactivity for p53 was evaluated and classified in two groups: '1', weakly or moderately positive (>5% to 20% positive cells); '2', strongly positive (>20%).

Immunostaining for p16 by TSA-IHC was classified in three groups: '0', negative; '1', positive in TSA-IHC (negative in IHC); '2', positive in standard IHC and TSA-IHC.

Mutational analysis by p53 GeneChip

Seven tumors were re-examined by the p53 GeneChip (Affymetrix). Tumor areas were microdissected similar to the standard sequencing procedure. The manufacturer's protocol was strictly followed, and according to an added on suggestion, the hybridization step was extended to 90 min in order to obtain a uniform hybridization intensity over all positions on the chip. Detailed description of the chip and the mixture detection algorithm used for mutation detection has been published (8, 10, 11).

Statistical analysis

For assessing statistical significance, Fisher's exact test and chi-square tests were used. Two-tailed analysis was performed, and *P*-values of <0.05 were considered statistically significant.

Results

We have analyzed 31 primary HNSCC. Most of the tumors were from the hypopharynx, oropharynx, and larynx, a few were from the oral cavity and nasopharynx. All of them showed an overexpression of the p53 protein in standard IHC but no mutation in sequence analysis of the exons 5–9 of TP53. These tumors were examined for AIs at TP53 and another 12 microsatellite markers dispersed over chromosome 17, and by IHC for expression of the p16^{INK4a} protein. A small number of the tumors were re-examined for p53 mutation with

Table 2 Summary of results of immunohistochemistry, allelotyping and p53 GeneChip analysis, relation to patient survival

ID	p53	p16	AI at TP53	> 1 AI/13	Mut	SM
101	1	0	1	1	+	13
542	1	0	1	1	+	102
685	2	0	1	1		35
185	2	0	1	1		101
383	2	0	1	1	+	156
317	2	0	1	1	+	99
157	1	0	1	1	+	105
294	2	0	1	1		13
343	1	0	1	1		24
509	2	0	1	1	+	96
475	1	0	1	1		68
688	2	1	1	1	-	16
275	1	1	1	1		148
644	2	1	1	1		15
299	2	1	1	1		108
385	1	1	1	1		152
397	2	1	1	1		20
481	2	0	0	1		44
592	2	0	0	1		34
510	2	1	0	1		105
426	1	1	0	1		159
97	2	1	0	0		164
499	1	2	0	0		62
551	2	1	0	0		11
672	2	1	0	0		52
66	2	1	0	0		138
595	2	1	0	0		17
693	1	1	0	0		33
63*	1	2	0	1		137
496*	1	2	0	0		103
689*	1	2	0	0		48
Total changes		13/31	17/31	22/31		

Cases with asterisk (*) have established HPV involvement (9, 10). p16 protein levels: 0 = negative, 1 = normal low level, 2 = high level; p53 protein levels: 1 = 5–20% positive cells, 2 = >20% positive cells; AI (allelic imbalance) at TP53: 0 = no, 1 = yes; > 1 AI/13: 0 = none or one allelic imbalance, 1 = more than one allelic imbalance (of 13 markers); Mut, re-examination of mutational status by the Affymetrix p53 GeneChip: + = mutation found, - = no mutation found; SM = survival in months; ID = patient identification number.

the p53 GeneChip. Table 2 summarizes the results of these analyses.

Analysis of p53 immunoreactivity by standard IHC

The first column after the patient ID in Table 2 shows the results of immunohistochemical staining for the p53 protein, taking into account the differentiation state of the tumors. They were classified into two groups: 41.9% (13 of 31) had a score of '1' (5–20% positive cells), 58.1% (18 of 31) had a score of '2' (>20% positive cells; see Figure 1a).

Analysis of the p16 immunoreactivity by IHC and TSA-IHC

Similar with p53, standard IHC does not allow the distinction between normal low level expression and loss or reduced expression of the p16 protein. Therefore, the 31 tumors were examined by TSA-IHC in addition to IHC for loss of p16. The immunohistochemical reactivity was classified in three groups: '0',

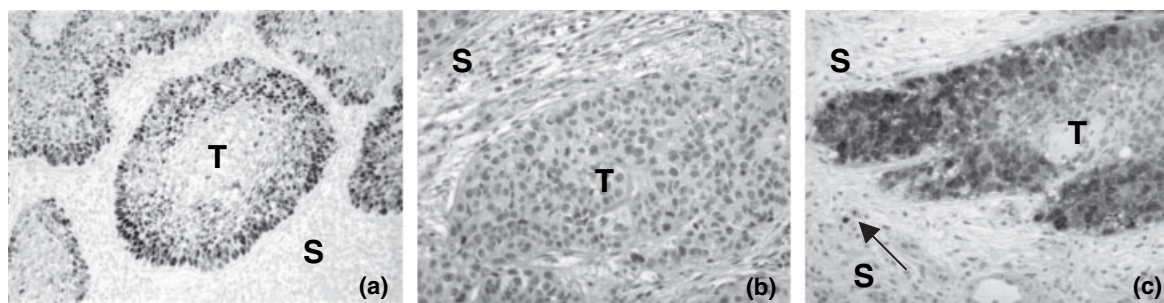


Figure 1 Immunohistochemistry (IHC) and tyramide signal amplification (TSA)-IHC for p53 and p16 in head and neck squamous cell carcinoma (HNSCC). (a) Positive IHC staining for p53 in a moderately differentiated oropharynx tumor, T2N0M0; (b) IHC; and (c) TSA-IHC for p16 in a poorly differentiated oropharynx tumor, T2N0M0. Conventional staining was negative (b), TSA-IHC revealed nuclear but also some cytoplasmic staining of tumor cells (c). Some stromal cells also turned positive for p16 (arrow). T, tumor; S, stroma.

negative after both IHC and TSA-IHC, '1', positive in TSA-IHC only (see Figure 1b and c); '2', positive in standard IHC. In 41.9% (13 of 31), a loss of the p16 protein was found (score 0).

Allelic imbalances at TP53 and other regions of chromosome 17

All 31 patients were informative for the 13 markers which were used to cover the length of chromosome 17. Most imbalances were found at *TP53*, amounting to 54.8% (17 of 31). All of these also showed imbalances at additional markers. About 71.0% (22 of 31) of the tumors showed an AI at more than one marker, but only five of them did not contain an imbalance at *TP53*. In contrast, nine tumors were normal at *TP53* and had maximally one imbalance at other loci (Table 2). Examples are shown in Figure 2.

Loss of p16 protein expression and its relationship with allelic imbalances

We examined the relationship between the loss of p16 protein expression and AI at the *TP53* locus and the other markers. About 13 of the 31 tumors (41.9%) displayed a loss of p16 protein. About 11 of them (84.6%) had imbalances at *TP53* (two had imbalances at other markers only). In contrast, of the 18 tumors with retained p16 protein expression, only six (33.3%) had *TP53* imbalances (five had AIs at few other loci only). Thus, there was a statistically significant association between loss of p16 and allelic loss of *TP53* ($P = 0.005$; Mantel-Haenszel chi-square, $P = 0.014$; Yates corrected). When we examined AIs at the other loci (without taking into account that the total numbers in the tumors with retained p16 expression were much lower), there was also a significant difference between the two groups ($P = 0.025$; two-tailed Fisher's exact test).

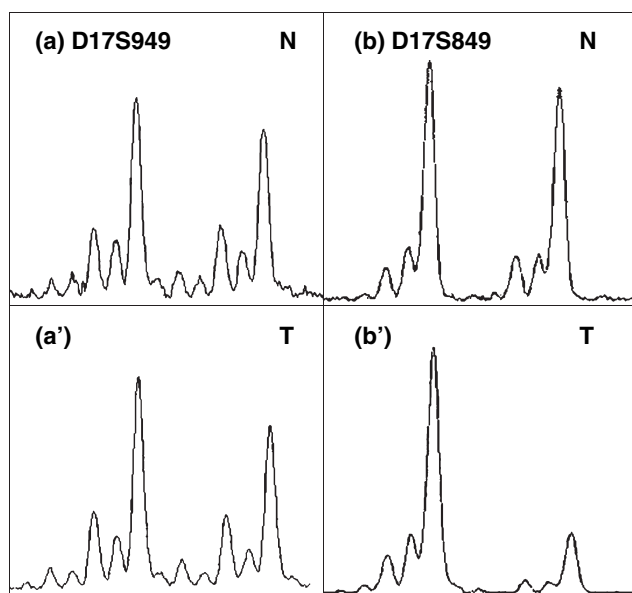


Figure 2 Examples of microsatellite marker analyses. D17S949 and D17S849 microsatellite markers have been analyzed; N, normal tissue; T, tumor tissue. (a, a') Tumor without allelic imbalance; (b, b') tumor with allelic imbalance. Note that there was no complete loss of one allele.

Analysis of p53 mutations by the p53 GeneChip

Seven tumors were re-examined by *p53 GeneChip*: six of them showed AIs at the *TP53* locus and at more than one other loci, and in addition had lost the p16 protein. They all revealed class II missense mutations ('structural mutations') that had not been detected by conventional sequencing. Importantly, all mutations were within the gene region previously examined. The *p53 GeneChip* confidence scores ranged from 15 to 20 and thus were in all six cases only marginally above the threshold score of 13 (8). These scores are compatible with the mutations being heterozygous rather than being present in only a subpopulation of tumor cells. Manual re-inspection of the electropherograms from dideoxy sequencing confirmed the presence of mutant peaks, which however were disregarded in all cases because of their low intensity. The seventh re-examined tumor also had AIs but had retained expression of the p16 protein. No mutation could be detected in this case.

The last column of Table 2 lists the survival times in months of the patients analyzed. As can be seen, the survival times were highly variable and did not correlate with the molecular parameters, neither when analyzed as single markers nor when analyzed in all possible combinations (data not shown).

Discussion

A substantial fraction of HNSCC display elevated levels of the tumor-suppressor protein p53, which however, appears to be wild type at least in the central core domain of the protein (exons 4–9). The functional status of p53 in these tumors, and its relationship with other biologic and with clinical parameters has remained unclear.

We used two parameters to re-examine the functional status of the p53 protein in these tumors. The first was the allelic status of the *TP53* locus on chromosome 17p.13, and the allelic status of other regions on chromosome 17. It is generally assumed that in tumors with the p53 gene being wild type, the incidence of AIs at *TP53* should be much lower than in tumors with mutated p53, and they should generally show a low frequency of imbalances on chromosome 17. The validity of this assumption is confirmed by the assessment of HNSCC associated with integrated papillomavirus (mostly HPV16) with active expression of the viral oncogenes E6 and E7. These tumors harbor a wild-type p53 gene (12–17). Because of the increased breakdown of the p53 protein induced by the E6 oncoprotein, there is no need to disrupt the p53 alleles. Microsatellite marker analysis of these tumors has revealed that they indeed display significantly less AIs at the *TP53* locus (7). In fact, they showed distinctly fewer AIs at a number of other loci including the *Rb* locus (12), in comparison to tumors without HPV involvement. The study presented here included three tumors with an established association with HPV16, reflected by the presence of viral DNA, E6 transcripts, reduced pRb staining (not shown), and accumulated p16^{INK4a} protein (labeled by asterisk in Table 2). None of these showed an AI at the *TP53* locus, and none or very few at the other chromosome 17 markers tested, in agreement with the data of Braakhuis et al. (7). In addition to the three HPV16-associated tumors, another 11 did not show AI at *TP53*. With one exception, these also showed none or only one alteration at the other markers. In these 14 of 31 tumors, the lack of AIs at *TP53* (and their scarcity at the other loci) supports the wild-type status of the p53 gene. In contrast, the presence of AI at *TP53* and the overall higher incidence of AI in the other tumors would suggest that these tumors carry genetic changes in *TP53* which could not be detected by routine sequencing of the central part of the gene.

As a second possible parameter for the functional status of p53, we examined the expression of the cyclin-dependent kinase 4/6 inhibitor p16^{INK4a}. This was based on two observations. First, the HPV-associated tumors (of the uterine cervix as well as of the tonsils and oropharynx) again serve as a paradigm for retained expression of p16^{INK4a} in tumors with wild-type p53 (12, 13). Because the pRb protein which is the central negative regulator of cell cycle progression is inactivated in these tumors by the viral E7 protein, the p16^{INK4a} protein accumulates but is no longer capable of inhibiting cell cycle progression. Secondly, in tumors with an intact pRb protein but an inactivated or lost p53 protein, loss or downregulated expression of p16^{INK4a} comprises

a major mechanism to abolish negative regulation of cell cycle progression by pRb. In line with this reasoning, we have observed a similar incidence of p16 loss and p53 alterations in HNSCC (18). The analysis of a large tumor cohort revealed that p53 alterations and loss of p16^{INK4a} showed a similar distribution between the different tumor sites and were directly associated (Karsai et al., 2005, personal communication). This led us to the hypothesis that p53 alterations and loss of p16^{INK4a} expression might be linked, e.g. by repression of DNA methyl transferases by p53, and relieve of repression upon p53 inactivation. About 13 of the 31 tumors examined here showed loss of expression of p16^{INK4a} which would suggest functional inactivation of p53. If p16^{INK4a} loss was a marker for genetic p53 alteration similar to AI at *TP53*, then the two parameters AI and p16^{INK4a} loss should also show positive rank correlations with each other. Of these 13 tumors, 11 had AI at *TP53*, whereas only six of the 18 tumors with retained expression of p16^{INK4a} had AI at *TP53* ($P = 0.013$; Yates corrected χ^2 -test). Similarly, all 13 tumors with p16^{INK4a} loss had more than one AI at the 13 chromosome 17 loci examined, whereas only nine of the 18 tumors with retained expression of p16^{INK4a} had more than one AI ($P = 0.0036$; two-tailed Fisher's exact test). These tests strongly suggested that most if not all of the tumors displaying both AI at *TP53* and p16 loss actually contained p53 mutations, which had gone unnoticed in our routine sequencing analysis using the dideoxy chain termination technique on the ABI 310 Genetic Analyzer.

Seven tumors with AI at *TP53* and more than one AI overall, one of which had retained expression of p16^{INK4a} were subjected to refined re-sequencing employing the *p53 GeneChip* from Affymetrix. All six tumors with negative p16 staining and AI revealed apparently heterozygous missense class II mutations, all of them located within the previously examined exons 5–8. This confirmed that AI and p16 loss are indicative of genetic damage of *TP53*. No p53 mutation could be found in the one tumor with retained p16^{INK4a} expression despite AI. Unfortunately, we could not re-examine further tumors by the Affymetrix *p53 GeneChip*, as it is no longer commercially available. Nevertheless, our data indicate that overexpression of p53 in HNSCC is more strongly associated with missense mutations than previously recognized: while p53 overexpression in our recently reported study had a predictive value of 72.5% for the presence of missense mutations, our present data result in a predictive value of higher than 86%, as about half of these tumors have AI at *TP53*, have lost the p16 protein, and have revealed heterozygous missense mutations. We conclude that examination of AI at *TP53* is a valuable adjunct method to determine the genetic status of p53 in HNSCC in cases with ambiguous sequencing results, and examination of p16 expression provides further support.

References

1. Landis SH, Murray T, Bolden S, Wingo PA. Cancer statistics, 1999. *CA Cancer J Clin* 1999; **49**: 8–31.

2. Hollstein M, Sidransky D, Vogelstein B, Harris CC. p53 mutations in human cancers. *Science* 1991; **253**: 49–53.
3. Ahomadegbe JC, Barrois M, Fogel S, et al. High incidence of p53 alterations (mutation, deletion, overexpression) in head and neck primary tumors and metastases; absence of correlation with clinical outcome. Frequent protein overexpression in normal epithelium and in early non-invasive lesions. *Oncogene* 1995; **10**: 1217–27.
4. Bosch FX, Ritter D, Enders C, et al. Head and neck tumor sites differ in prevalence and spectrum of p53 alterations but these have limited prognostic value. *Int J Cancer* 2004; **111**: 530–8.
5. Cho Y, Gorina S, Jeffrey PD, Pavletich NP. Crystal structure of a p53 tumor suppressor-DNA complex: understanding tumorigenic mutations. *Science* 1994; **265**: 346–55.
6. Mao L, Lee JS, Fan YH, et al. Frequent microsatellite alterations at chromosomes 9p21 and 3p14 in oral premalignant lesions and their value in cancer risk assessment. *Nat Med* 1996; **2**: 682–5.
7. Braakhuis BJ, Snijders PJ, Keune WJ, et al. Genetic patterns in head and neck cancers that contain or lack transcriptionally active human papillomavirus. *J Natl Cancer Inst* 2004; **96**: 998–1006.
8. Ahrendt SA, Halachmi S, Chow JT, et al. Rapid p53 sequence analysis in primary lung cancer using an oligonucleotide probe array. *Proc Natl Acad Sci U S A* 1999; **96**: 7382–7.
9. Kropveld A, Rozemuller EH, Leppers FG, et al. Sequencing analysis of RNA and DNA of exons 1 through 11 shows p53 gene alterations to be present in almost 100% of head and neck squamous cell cancers. *Lab Invest* 1999; **79**: 347–53.
10. Wikman FP, Lu ML, Thykjaer T, et al. Evaluation of the performance of a p53 sequencing microarray chip using 140 previously sequenced bladder tumor samples. *Clin Chem* 2000; **46**: 1555–61.
11. Wen WH, Bernstein L, Lescallett J, et al. Comparison of TP53 mutations identified by oligonucleotide microarray and conventional DNA sequence analysis. *Cancer Res* 2000; **60**: 2716–22.
12. Andl T, Kahn T, Pfuhl A, et al. Etiological involvement of oncogenic human papillomavirus in tonsillar squamous cell carcinomas lacking retinoblastoma cell cycle control. *Cancer Res* 1998; **58**: 5–13.
13. Wiest T, Schwarz E, Enders C, Flechtenmacher C, Bosch FX. Involvement of intact HPV16 E6/E7 gene expression in head and neck cancers with unaltered p53 status and perturbed pRb cell cycle control. *Oncogene* 2002; **21**: 1510–7.
14. van Houten VM, Snijders PJ, van den Brekel MW, et al. Biological evidence that human papillomaviruses are etiologically involved in a subgroup of head and neck squamous cell carcinomas. *Int J Cancer* 2001; **93**: 232–5.
15. Herrero R, Castellsague X, Pawlita M, et al. (IARC Multicenter Oral Cancer Study Group). Human papillomavirus and oral cancer: the International Agency for Research on Cancer multicenter study. *J Natl Cancer Inst* 2003; **95**: 1772–83.
16. Hafkamp HC, Speel EJ, Haesevoets A, et al. A subset of head and neck squamous cell carcinomas exhibits integration of HPV 16/18 DNA and overexpression of p16INK4A and p53 in the absence of mutations in p53 exons 5–8. *Int J Cancer* 2003; **107**: 394–400.
17. Dai M, Clifford GM, le Calvez F, et al. (IARC Multicenter Oral Cancer Study Group). Human papillomavirus type 16 and TP53 mutation in oral cancer: matched analysis of the IARC multicenter study. *Cancer Res* 2004; **64**: 468–71.
18. Grütgen A, Reichenzeller M, Junger M, Schlien S, Affolter A, Bosch FX. Detailed gene expression analysis but not microsatellite marker analysis of 9p21 reveals differential defects in the INK4a gene locus in the majority of head and neck cancers. *J Pathol* 2001; **194**: 311–7.

Acknowledgments

The authors greatly acknowledge the excellent technical help from Antje Schuhmann, Stefanie Huntgeburth, and Wolfgang Klein-Kühne and would also like to thank Dr C. Flechtenmacher, Pathologisches Institut der Universität Heidelberg (for histopathologic assessment and discussions), and Dr U. Abel, Zentrum für Medizinische Biometrie und Informatik, Universität Heidelberg (for help with statistical analysis).

This document is a scanned copy of a printed document. No warranty is given about the accuracy of the copy. Users should refer to the original published version of the material.